This document was prepared in conjunction with work accomplished under Contract No. DE-AC09-76SR00001 with the U.S. Department of Energy.

DISCLAIMER

TECHNICAL DIVISION
SAVANNAH RIVER LABORATORY

DPST-81-828

CC: J. R. Hilley, SRL
J. A. Porter
J. G. Smith
E. L. Wilhite
M. H. Tennant
H. B. Peacock, Jr.
J. D. Stewart
A. Gibbs
J. R. Cadieux
R. S. Swingle, SRP
J. H. Owen
P. T. Deason
R. S. Thomason
R. L. Frontroth
TIS File (2)

ACC. NO. 140197

M E M O R A N D U M

November 10, 1981

TO: M. L. HYDER/D. A. WARD

FROM: W. G. WINN/E. T. BOOTH

TIS FILE
RECORD COPY

APPRAISAL OF ACTIVE WELL COINCIDENCE COUNTER FOR URANIUM ACCOUNTABILITY

I. Introduction

The Active Well Coincidence Counter (AWCC) is a relatively inexpensive ($50K) instrument for monitoring fissile materials.[1-7] Currently, SRL/SRP relies heavily on the more expensive ($500K) Cf shuffler in 300-Area for such interrogation.[8-9] Because the AWCC provides a quick non-destructive assay, it also has advantages over other methods in use, such as mass spectroscopy. Thus, the FAB lab has coordinated recent feasibility studies on the AWCC. These follow earlier studies on billet samples at 300-Area[5,10,11], and include: (1) U_3O_8

powders received at the FAB lab[12], (2) two low-mass uranium standards provided by New Brunswick Laboratories[13-14], and (3) scrap can samples from 300-Area[15-16]. These samples ranged from 0 to 7 Kg in ^{235}U. It was desirable to see whether the AWCC could make assays to 1% accuracy.

The AWCC, developed at LASL, uses two AmLi sources to produce fissions in a sample with uranium. The resulting fission neutrons are detected in coincidence at a rate governed by the amount of ^{235}U in the sample. The count rates provide ^{235}U assays with statistical accuracy to <1%, in less than an hour of counting, but systematic errors require examination for complete appraisal.

This study emphasized the AWCC capabilities for the U_3O_8 powder samples, which ranged up to 12 Kg in mass and 93% in ^{235}U enrichment. In particular, it was desired to (1) identify and correlate the sample parameters which were sensitive to count rate, and (2) appraise the reliability of measurements with the AWCC. For the other types of samples, which had less ^{235}U, the projected measurement errors were much larger than 1%, and detailed parameter tests were not performed.

II. Summary

These studies demonstrated an AWCC measurement capability accurate to ~2% at 95% confidence level, for Kg amounts of ^{235}U in U_3O_8 powder. This performance corresponded to count times of 2000 sec. A careful study of the measurement errors projected that the accuracy may be improved to 1% with suitable controls. The demonstrated accuracy was considerably worse for samples having <1 Kg ^{235}U. Also, the scrap sample measurements may have been affected by sample inhomogenieties.

A good empirical fit to the U_3O_8 powder data was obtained and could be interpreted physically. This indicates that Monte Carlo[5,17] calculations for the AWCC could be used to reduce the effort required for producing AWCC calibration data.

III. Experimental Aspects

A. AWCC Description

The AWCC measures the amount of ^{235}U in a sample by monitoring the fission rate induced by two AmLi (α,n) neutron sources. Each source has 0.71 gm ^{241}Am and produces $1.7X10^5$ n/sec.[18] A block diagram of the instrumentation is

shown in Figure 1. Detailed information on the AWCC is available.[1,3]

The sample is placed in a central cavity of a 19" diameter by 24" high polyethylene barrel. The two AmLi sources are situated just above and below the sample so that the sample is irradiated reasonably uniformly with fast neutrons. Cadmium shielding about the sources, as shown in Figures 2 and 3, reduces non-uniform sample irradiation by thermal neutrons. In addition, an annular nickel reflector about the center of the cavity enhances the more penetrating irradiation of fast neutrons in the sample. The n-irradiated sample produces fissions which release several neutrons per a single fission. These fission neutrons are correlated per a given fission; thus, detection of two or more neutrons in coincidence yields a measure of the fission rate or ^{235}U content.

The neutrons are detected by 42 ^{3}He detectors which are located in an outer annulus of the polyethylene barrel, as shown in Figure 1. Each detector has 1 in. diameter and 20 in. length. Cadmium shielding about the inner and outer surfaces of the detector annulus reduces the neutron background from the AmLi sources and the room, and thus helps reduce the random coincidence background from these effects. The polyethylene within the detector annulus helps thermalize the fission neutrons so that the ^{3}He-detector efficiency is enhanced.

The detection electronics is also shown in Figure 1. A single high voltage (1500 V) supply is connected to all 42 ^{3}He detectors. The detector outputs are ganged in 6 groups of 7 detectors each. Each detector group has its own preamp, amplifier, and level discriminators, so that the effects of pileup are reduced. The shorter duration discriminator output pulses of each group are passed through an OR gate and then into a shift-register coincidence counter (SRCC).[3,19] The SRCC electronically stores, in a special counter, each neutron pulse for a time interval (64 μ sec)* for which most real (fission) coincidences should occur. In addition, each neutron pulse strobes this counter just before its storage in counter and then $\sim$1000 μ sec after its departure from counter. The immediate strobe obtains the real (R) plus random (A) coincidence in the counter, while the delayed strobe obtains only the random coincidences (A) in the counter. The accumulated R+A and A for a given count time t, as well as the total neutron count T, are tallied by a microprocessor. After counting, the data in the microprocessor are passed to a HP-97 programmable calculator.

---

* The maximum total count rate is usually < $1/64\mu$ sec or 15,000/sec

A code then calculates T, R+A, A, t, R and asociated counting errors.†

B. Samples

U_3O_8 Powder Samples The U_3O_8 powder samples ranged from 2 kg to 12 kg, with ^{235}U enrichments from 0.17% to 93%, as summarized in Appendix Tables A.1-A.4[12]. Various of these samples were contained in three different types of steel cans. Dimensions for these cans and the corresponding AWCC counting geometries are given in Figures 2 and 3.

Scoping studies used the AWCC geometry of Figure 2. Either oxide storage cans (OSC) or #10 cans contained the sample. Each OSC container had a polyurethane top and was enclosed in a polyethylene bag. Each #10 can was sealed with a metal lid and thus required no outer polyethylene bag; however, the U_3O_8 was contained within a polyethylene bag inside each can. Data obtained for these samples are detailed in Appendix Tables A.1 and A.2.

The detailed studies used the AWCC geometry of Figure 3. Only #10 cans were used in this case. Each #10 can had a polyurethane top and was enclosed in a polyethylene bag. No polyethylene bag was used inside the can. Five #10 cans with 12.00 Kg of U_3O_8 of different enrichment were prepared and counted in the AWCC. Then 2.00 Kg from each of these cans were placed in five additional #10 cans, whereby cans of 10.00 Kg and 2.00 Kg were counted. Similarly, these cans were remeasured for 8.00 and 4.00 Kg samples and finally, for 6.00 Kg and 6.00 Kg. This procedure resulted in the data summarized from detailed data in Appendix Tables A.3 and A.4. in Table I. The 6.00 Kg samples were counted repeatedly, on various days, to yield detailed information on measurement reproducibility. A 12.00 Kg depleted sample was also counted.

New Brunswick Samples The two New Brunswick Laboratory samples[13-14] each had a net weight of 950 gm, contained in a 3 3/8"-diameter X 8" tall polypropylene can. One sample had no ^{235}U and the other had 125.35 gm of ^{235}U of a total of 134.78 gm U, as indicated in Appendix Table A.5. Each sample was counted, using the AWCC geometry of Figure 3.

† An RS-232 output is also available on the microprocessor.

300-Area Scrap Samples The scrap uranium samples[15-16] were 300-Area "floor sweepings." In all, there were six samples ranging from 140 to 420 gm of ^{235}U, as shown in Appendix Table A.6. Each of these samples was contained in a "short" #10 can* and counted in the AWCC geometry of Figure 3.

C. Measurement Techniques

Before introducing any sample into the AWCC, the instrument settings described in Section IIIA were confirmed. Upon daily power up, the AWCC measured (1) the background to check that it was zero within statistics, and (2) a U_3O_8 sample counted previously to confirm that the AWCC was calibrated consistently.**

Each sample was counted for at least two 500 sec intervals to check that instrument drifts were insignificant with respect to the counting statistics. Such drifts can be caused by temperature/humidity, line voltage, and similar effects. Efforts were made to minimize these. Each U_3O_8 sample in the scoping measurements was counted for at least two 500 sec consecutive intervals, and all other samples were counted for at least four 500 sec consecutive intervals.

IV. AWCC Appraisal Studies with U_3O_8 Powders

A. Preliminary Scoping Studies

Initial tests with U_3O_8 samples in #10 and OSC cans, counted in AWCC geometry of Figure 2, were useful in defining parameters sensitive to neutron count rate R. It would have been ideal if R were directly proportional to the mass of U-235, or

$$R = C'm \qquad (1)$$

---

* About 1" shorter than #10 can in Figure 2, and having a metal seal top (no polyurethane).

** During operator breaks, power down/up occurred sometimes during the day

The scoping measurements (tabulated Appendix Tables A.1 and A.2) for the #10 and OSC samples show that equation (1) is approximately correct, as indicated in Figure 4. However, when plotting these results as R/m = C' vs. m, as shown in Figure 5, C' is seen to be a decreasing function of m. This implies that larger amounts of U-235 have more self-shielding relative to the AmLi neutron sources, which in turn reduces the fission rate per Kg of U-235 (or effectively, R/m).

Further examination of Figures 4 and 5 indicates that various data for these plots deviate significantly from any smooth average curves that represent the overall trends. However, uniform trends did exist for points having similar enrichment e, as indicated in the figures. Thus, in addition to the m dependence, C' is also dependent on e. Therefore, we can write

$$R = C'(m,e)m \qquad (2)$$

It should be noted that a different C'(m,e) will result for different types of U_3O_8 containers in general, although no measurable effect was observed in these scoping studies. C'(m,e) may also depend weakly on the U isotopics other than U-235, but these were not isolated in the present studies.[8] Thus, we proceed to examine the m and e dependences alone.

For an unknown sample, the enrichment e will not usually be known; however, the total mass M of U_3O_8 may be determined by weighing. Furthermore, because

$$e = a(m/M) = af \qquad (3)$$

where

$$a = U_3O_8 \text{ mol wt}/U_3 \text{ mol wt}$$

$$f = m/M$$

we may write

$$C' = C'(fM,af) = C(M,f)$$

- or -

$$R = C(M,f)m = C(M,f)Mf \qquad (4)$$

Thus, by measuring R and M, we can calculate f to obtain m = Mf, provided that C(m,f) has been established from calibration studies.

The detailed studies that follow were aimed at appraising whether equation (4), deduced via the above scoping studies, can be usefully defined for AWCC determination of U-235 in U_3O_8 powders.

B. Detailed Calibration Studies

Measurements for samples of known U_3O_8 and enrichment in #10 cans were designed to establish how well equation (4) could be calibrated. Cans with M = 2.000, 4.000, ------, and 12.000 Kg of U_3O_8 and with f = 0.329, 0.411, 0.494, 0.578, and 0.646 were studied. A can with depleted U_3O_8 (M=12.00, f=0.0014) was also studied. The data for these measurements are given in Table I (see Appendix Tables A.3 and A.4 for details). The AWCC counting geometry† and R vs. m results are given in Figures 3 and 6. The results compare reasonably with those from the scoping studies shown in Figure 4. The results that test equation (4) directly are shown in Figure 7, where R vs. f is given for each M.

The smooth curves in Figure 7 are fits to the data and are given by

$$R = 153.3(1+1.214e^{-f/0.278})(1+0.535e^{-M/3.28})MF \qquad (5)$$

where

R is in counts/sec
M is in Kg
f is unitless

In addition, it is seen that equation (5) is equation (4) with

$$C(M,f) = 153.3(1+1.214e^{-f/0.278})(1+0.535e^{-M/3.28}) \qquad (6)$$

Equation (6) for C(M,f) was deduced by examining the measured C(M,f) = R/Mf values summarized in Table II. The data suggest that C(M,f) has a functional form of $c_1(M)c_2(f)$.†† To deduce the best representation of $c_1(M)$ and $c_2(f)$, the C(M,f) data were combined into the averages,

$c_1(M) = \underline{C(M,f)}$, average of 5 f-cases for each M
$c_2(f) = \overline{C(M,f)}$, average of 6 M-cases for each f

† This geometry was somewhat different from that of Figure 2, because the polyurethane lid was included.

†† By contrast, C(M,f) was shown to be poorly represented by a functional form C(Mf) = C(m).

The resulting $c_1(M)$ and $c_2(f)$ data are plotted in Figures 8 and 9, and are fitted to the expressions:

$$c_1(M) = 187.7\ (1+0.535e^{-M/3.28}) \qquad (6a)$$

$$c_2(f) = 168.9\ (1+1.214e^{-f/0.278})$$

The constant factors in front of these expressions are dependent on the f or M values included in the averages, but the relative M or f dependencies given by the second factors are independent of the averaging method. Thus, we may write

$$C(M,f) = C_o(1+1.214e^{-f/0.278})(1+0.535e^{-M/3.28})$$

- or -

$$C_o = \frac{C(M,f)}{(1+1.214e^{-f/0.278})(1+0.535e^{-M/3.28})} \qquad (6b)$$

By calculating a C_o for each of the 30 (M,f)-cases, as shown in Table III, an average $\bar{C}_o = 153.3 \pm 0.4$ was obtained.

The individual C_o values are distributed about $\bar{C}_o$ with a standard deviation of 1.4%. As shown in Table IV, over half of the C_o deviate from $\bar{C}_o$ by <1%, but several larger deviations (max of 2.9%) tend to raise the overall standard deviation. It is suspected that some of these larger deviations are associated with instrument instabilities†, which may be reducible. Upon close examination, one should recognize that the %-deviations of C_o from $\bar{C}_o$ are also the corresponding %-deviations between the measured R values and those obtained with equation (5).

The nature of equation (5) suggests some theoretical dependencies that might be refined by neutron transport or Monte Carlo calculations.[5,17] To a large degree, the count rate R is proportional to the ^{235}U mass m = Mf. However, this mass is shielded from neutrons by a factor of $(1+1.214e^{-f/0.278})$ due to enrichment effects and a factor of $(1+0.535e^{-M/3.28})$ due to overall mass M. The exponential term in each factor is probably associated with the thermal neutron flux attenuation. The other term is constant (unity) and thus, is probably associated with the fast neutron flux, which is only weakly attenuated. Although the above two-group neutron flux treatment yielded a good model for R, as given by equation (5), a multi-group analysis might improve the curve fitting. A correction for isotopic effects on count rate could be included also.[8]

† Instabilities caused by temperature-humidity conditions, power line fluctuations, etc.

Possible isotopic effects may have been observed in the depleted U_3O_8 sample, where the observed count rate of 20.4 ±1.8/sec is noticeably larger than the 5.9 c/sec predicted by equation (5).

C. Reliability of the Method

The reliability of measuring ^{235}U mass m with the AWCC was appraised in terms of the precision and accuracy of the R measurements. The detailed analysis involved numerous measurements for #10 cans containing M = 6.000 Kg of U_3O_8 powder. Also, the agreement of R measurements with the predictions of equation (5) are used.

The precision was examined for errors caused by counting statistics and sample distribution. The results for the M = 6.000 Kg series of measurements (distributed over one month) are given in Figure 10. Data related to the comparison with equation (5) are given in Table IV.

In Figure 10a, the standard deviation of R due to counting statistics σ_S is compared with the total standard deviation σ_T, calculated as

$$\sigma_T = \sqrt{\sum_n (R-\bar{R})^2/n-1} \qquad (7)$$

where

$\bar{R}$ = average of R-measurements
n = number of R-measurements

Agreement between σ_T and σ_S is reasonably good, suggesting that counting error is dominant in the present measurements.† For one case, σ_T was significantly larger than σ_S; however, removing one deviant set of measurements resulted in much better agreement for this case. A detailed analysis of these measurements, relative to confidence levels, is given in Table V and Appendix Table A.4. The average σ_T error in R was 0.69%, yielding a 95% confidence level error of 1.35%. The corresponding average σ_S error is 0.57%, yielding a 95% confidence level error of 1.12%. The 1-σ error, excluding counting statistics, is given by

† R was measured with 2000 sec count times. For sufficiently longer count times, σ_S may decrease relative to σ_T.

$\sigma_o = \sqrt{\sigma_T^2 - \sigma_S^2} = 0.39\%$, which would be $\simeq \sigma_T$ for count times >10X longer than 2000 sec. This σ_o represents the ultimate precision one might expect from these studies.

In Figure 10b, two separate series of measurements, labeled E and F, are compared. As each separate series involved measurements for identical samples (same M and f values), taken under similar conditions, these results were used to appraise whether E and F fluctuations are correlated with laboratory conditions. In Figure 10b, the suspected correlated E and F values† of $\Delta R = R - \bar{R}$ are plotted against each other. The correlation coefficient for these data was calculated as

$$\rho = \frac{\sum (R(E)-\bar{R}(E))(R(F)-\bar{R}(F))}{(n-1)\sigma(E)\sigma(F)}$$

where

$R(X)$ = count rate for series X measurement.
$\bar{R}(X)$ = count rate for series X average.
$\sigma(X)$ = standard deviation for X in Figure 10b.
n = number of points in Figure 10b.

The resulting $\rho = 0.3$ indicates that a weak correlation did exist. Probably drifts in detector efficiency due to temperature-humidity effects, detector voltage setting, etc. are contributing to the overall correlation. Later measurements in this series addressed some of these effects, suggesting that ρ can be kept small so that the uncorrelated statistical counting error will dominate. Correlated errors can also be reduced by daily normalization corrections using a known standard U_3O_8 sample.

In Figure 10c, the sample-to-sample precision of purported identical (M,f)-cases for E and F series measurements are appraised. Here $\Delta = R(E)-R(F)$ are compared. Agreement between Δ and 0.0 is good, being distributed within $2\sigma_\Delta \approx 0.5\%$ of the measurement error.††. Thus, no noticeable additional error was exhibited for sample preparation effects such as weighings, can geometry consistency, etc.

---

† Values measured within a few hours of each other

†† $\sigma_\Delta = \sqrt{\sigma_T^2(E)/n(E) + \sigma_T^2(F)/n(F)}$, where σ_T and n are defined in equation (6).

The accuracy was investigated by assuming that systematic errors are given by deviations from a smooth fit to the R vs f plot for the well-studied M = 6.000 Kg data.† The statistical average of the 14 or 15 measurements for each point has a statistical error of <0.3%. Deviations beyond this are systematic in part. As shown in Figure 11, such deviations are <1%, and the average RMS deviation is 0.6%.

The above examination of precision and accuracy suggests what may be feasible under optimal measurement conditions. The overall precision and accuracy demonstrated by the present work is not considered optional, but was estimated by examining the average deviation in C_o (equivalently R) for each M or f, as shown in Table IV. These average deviations, $DC_o \pm \sigma(DC_o)$, are used to estimate accuracy with the DC_o values and precision with the $\sigma(DC_o)$ values. The DC_o, which are averages of C_o deviations from equation (5), should be 0.0% if systematic errors are absent.

The DC_o values are from -0.9% to +0.9%, and have a RMS average of 0.60%. The $\sigma(DC_o)$ values range from 0.5% to 2.0%, with an RMS average of 1.3% (corresponding to 95% confidence level of 2.5%).

In sum, it is seen that all measurements of R are consistent with having a systematic error of $\sim$0.6%, and that statistical errors can be reduced well below 1% with suitable counting times and good measurement conditions.

The reliability for m measurements must be deduced from the precision and accuracy of the R measurements. Assuming that reliable accuracy can be afforded with a good set of calibration standards, the above discussion implies that, under good measurement conditions, the limiting error will be governed by the counting statistics. The discussion that follows will apply to the 2000 sec counts used in this study.

The statistical precision for R measurements is summarized in the σ_S vs R plot of Figure 12. Here, the counting error σ_S is relatively insensitive to true coincidence rate R, because R is the difference in two large count rates - the "trues plus randoms"

† The M = 6.000 Kg data above yield C_o = 154.6, per fit to equation (5).

minus "randoms". By setting $\sigma_R = \sigma_S$, we predict the standard deviation σ_m in the ^{235}U measurement as

$$\sigma_m = \sqrt{\left(\frac{\partial m}{\partial R}\sigma_R\right)^2 + \left(\frac{\partial m}{\partial M}\sigma_M\right)^2}$$

$$\sigma_m \approx \frac{\partial m}{\partial R}\sigma_R \qquad (7)$$

where the error σ_M in the total U_3O_8 is small. A more convenient representation of equation (7), is

$$\sigma_m = \frac{\partial m}{\partial R}\sigma_R = \frac{\partial (fM)}{\partial R}\sigma_R = \frac{M\sigma_R}{\partial R/\partial f}$$

- Or -

$$\frac{\sigma_m}{m} = \frac{\sigma_R}{f\ \partial R/\partial f} \qquad (8)$$

By differentiating equation (5) for $\partial R/\partial f$, we obtain

$$\frac{\sigma_m}{m} = \frac{\sigma_R}{R}\left(1-\frac{1.214(f/0.278)}{e^{f/0.278}+1.214}\right)^{-1} \qquad (9)$$

The σ_m/m results are plotted against m in Figure 13. A quick appraisal of equation (8) shows that the % errors σ_m/m and σ_R/R are not too different, since $f\partial R/\partial f \approx R$ from equation (9) and Figure 4.† This provides a useful guide for appraising the counting statistics required for a given ^{235}U measurement.

Figure 13 indicates that measurements for m>1.0 Kg can be made to precision of 1% with 2000 sec counts, but the error increases rapidly for smaller m. The results also indicate that measurements for a large sample are preferable to summing the measurements of smaller components of this sample, as the accuracy and counting times are more favorable. (In effect, each component contributes its own random-coincidence background, so that the

† A detailed analysis using equation (9) shows $0.67R < f\frac{\partial R}{\partial f} < R$.

total background correction error is larger.) This contrasts with the typical low-background nuclear statistical error, where either approach yields essentially the same error.† Theoretical correlations for the statistical errors have been developed.[6]

V. AWCC Measurements on Test Samples

A. U_3O_8 Powder Samples

A test U_3O_8 sample in a #10 can was weighed (M = 10.225 Kg) and counted in the AWCC (R = 730.3±3.4/sec = average of four 2000 sec counts). Using equation (5), values of f = 0.333±0.002 and m = 3.406±0.023 Kg were calculated, where the errors correspond to the counting error above.

Mass spectroscopy measurements for the same sample indicate m=3.347±0.021 Kg, which differs from the AWCC value by 1.7±0.9%, which is consistent with the deviations shown in Table IV. Thus, the AWCC and mass spec values agree to within 2σ = 1.8%.

The above result implies that equation (5), which is used to calculate m, is not accurate enough to assure m determinations accurate to $\sim$1% with 95% confidence level. However, it appears that improved techniques, using a combination of measurements and Monte Carlo calculations,[5,17] can provide better calibration curves, as well as reducing the number of calibration measurements required.

B. New Brunswick Test Samples

Results for the NBL samples are given in Appendix Table A.5. The 2000 sec measurements of each the 0.0 gm and 125.35 gm ^{235}U samples yielded -8±4 gm and 140±7 gm, where the errors are σ_S. (The corresponding σ_T were respectively ±14 gm and ±20 gm.) These results were calculated using equation (5). Although agreement is reasonable with respect to σ_S and σ_T, the associated %-error is >10%, which is not surprising in view of the

---

† Assuming we get $N \pm \sqrt{N}$ counts for a sample in time t, we break the sample into n smaller samples and obtain $N_i \pm \sqrt{N_i}$ counts for the ith sample in time t. The total count for all n samples is then

$$\Sigma(N_i \pm N_i) = (\Sigma N_i) \pm \sqrt{\Sigma(\sqrt{N_i})^2} = (\Sigma N_i) \pm \sqrt{\Sigma N_i}$$

$$N \pm \sqrt{N}$$

error projected in Figure 13. On the other hand, the above agreement is better than that reported earlier for these measurements,[14] prior to the development of equation (5).

C. 300-Area Scrap Samples

The AWCC measurements for the 300-Area scrap samples are summarized in Appendix Table A.6. Each sample was measured with four 2000 sec counts. The ^{235}U content was then determined using equation (5). The AWCC values for the two heavier samples agreed to ∿2% of the known ^{235}U content, but the AWCC values for the four lighter samples were all low by 20-40%.

It is questionable whether the data were reliable for the four lighter samples, as σ_T for each was considerably larger than σ_S, suggesting unstable operating conditions. Some of the measurements for each of these samples were taken on the same date; however, a calibration measurement on this date reproduced the count rate obtained earlier for a 6.00 Kg sample. Because each sample was not moved during the four 2000 sec counts, the σ_T should not have been dramatically larger than the σ_S.

The questionable low count rates may have resulted in high voltage breakdown in the detectors. Thus, assuming that the largest 2000 sec count rate for each sample may have been more representative, the results were recalculated, as shown in Table A.6. The agreement was within 15% for all cases except one (which disagreed by 26%), but all values were still low. It may be that geometrical distribution effects of the ^{235}U in the sample are being noticed. A future reexamination of these or similar samples is needed to completely resolve these discrepancies.†

VI. Conclusions

These studies demonstrate a feasibility for using the AWCC to measure ^{235}U ($m > 1$ Kg) in U_3O_8 to an accuracy of ∿1%, provided that stable measurement conditions are maintained and that calibration curves defined by equation (3) have been established for the AWCC counting geometry used. This performance may be accomplished with several 2000 sec counts of a sample; however, good temperature, humidity, and electrical conditions should be assured by calibration tests with a standard sample of U_3O_8.

† Unfortunately, the AWCC had been scheduled for return to LASL before these discrepancies were fully appreciated.

The performance was not as good for the New Brunswick standards and the 300-Area scrap samples.[13-16] In these cases, with ^{235}U < 1 Kg, a 2000 sec count yielded significantly worse accuracy. For example, a 400 gm sample would be measured with a 1- precision of only 3%, and a counting time of at least 18,000 sec or 5 hrs would be required to improve the precision to 1%. For smaller samples, the situation is even more severe. Also, for nonuniform samples, the shielding effects can cause systematic errors, which were not examined in this work. Thus, the described method is not strongly recommended for measuring samples with 500 gm, or samples with known non-uniformities in shielding. On the other hand, the method has been modified to work better for low ^{235}U samples, by removing the Cd shielding to improve the thermal neutron fission rate.[2,7] However, any effects due to non-uniformities would be increased with the more absorbant thermal neutrons. Overall, the method works best for large samples of ^{235}U, both in terms of accuracy and counting times.

References

1. Howard O. Menlove, "Description and Operation Manual for Active Well Coincidence Counter," Los Alamos Scientific Laboratory report LA-7823-M (May 1979).

2. H. O. Menlove, N. Ensslin, C. R. Hatcher, E. Medina, and J. Foley, "Active Well Coincidence Counter," Los Alamos Scientific Laboratory report LA-7211-PR (1977) pp. 7-10.

3. Merlyn Stewart Krick and Howard O. Menlove, "The High-Level Neutron Coincidence Counter (HLNCC): Users' Manual," Los Alamos Scientific Laboratory report LA-7779-M (1978).

4. Howard O. Menlove, Norbert Ensslin, and Thomas E. Sampson, "Experimental Comparison of the Active Well Coincidence Counter with the Random Driver," Los Alamos Scientific Laboratory report LA-7882-MS (June 1979).

5. Howard O. Menlove and Gerald E. Bosler, "Application of the Active Well Coincidence Counter (AWCC) to High-Enrichment Uranium Metal," Los Alamos Scientific Laboratory report LA-8621-MS (August 1981).

6. J. E. Swansen, N. Ensslin, M. S. Krick, and H. O. Menlove, "A New Shift Register for High Count Rate Coincidence Applications," Los Alamos Scientific Laboratory report LA-6788-PR (1977).

7. Nuclear Safeguards Research Program Status Report, January - March 1979, Los Alamos Scientific Laboratory report LA-7801-PR (June 1979), p. 42-44.

8. T. W. Crane, "Test and Evaluation Results of the ^{252}Cf Shuffler at the Savannah River Plant," Los Alamos Scientific report LA-8755-MS (March 1981).

9. J. H. Owen (Memorandum to S. P. Rideout), "Californium Shuffler," June 15, 1981.

10. N. Ensslin, P. Collinsworth, W. L. Belew, R. S. Thomson, and P. Deason, "Uranium Assays at SRP with the AWCC Neutron Detector," (in preparation).

11. Nuclear Safeguards Research Program Status Report, July - Sept 1980, Los Alamos Scientific Laboratory report LA-8590-PR (March 1981), p. 21-23.

12. H. B. Peacock, "Powder Metallurgy at Savannah River Laboratory," DP-1524 (December 1978).

13. Letter, N. H. Seebeck to J. H. Owen, "Measurement of U-235 Content in NBL Standards," June 5, 1981.

14. E. T. Booth (memorandum to Ann Gibbs), "Evaluation of New Brunswick Standards with Active Well Coincidence Counter," July 23, 1981

15. J. H. Owen (memorandum to R. S. Swingle, II), "U-235 for SRL Evaluation of AWCC," May 21, 1981.

16. RTA No. 1-SP/SG, "Additional Evaluation of AWCC for Assay of ^{235}U in Small Quantity (25 to 400 gm)."

17. Gerald E. Bosler, "Analytical Techniques to Reduce the Number of Physical Standards Needed for Neutron Coincidence Counter," Los Alamos Scientific Laboratory report LA-8509-MS (July 1981).

18. E. T. Booth (memorandum to D. A. Ward), "Safety Evaluation of Active Well Coincidence Counter," DPST-81-337, March 24, 1981.

19. James E. Swanson, Paul R. Collinsworth, and Merlyn Krick, "Shift Register Coincidence Electronics System for Thermal Neutron Counter," Nuclear Instruments and Methods 176 (1980), 555-565.

TABLE I. COUNT RATE R FOR U_3O_8 MEASUREMENTS[a]

M=mass U_3O_8 (Kg)	f=weight fraction of ^{235}U				
	.3285	.4106	.4940	.5777	.6464
12.0	848.9	953.6	1116.3	1257.1	1348.2
10.0	703.0	815.3	929.2	1036.5	1141.3
8.0	570.8	671.1	765.5	852.1	903.1
6.0	455.8	524.0	600.3	675.5	726.0
4.0	325.8	373.3	433.2	460.3	512.9
2.0	174.8	203.5	239.8	271.1	287.2

R values in counts/sec[b]

a) Detailed studies, using AWCC geometry of Figure 3.

b) R measured using ≥2000 sec count time. See Appendix Tables A.3 and A.4 for details.

TABLE II. R/Mf FOR U_3O_8 MEASUREMENTS

M=mass U_3O_8 (Kg)	f=weight fraction of ^{235}U .3285	.4106	.4940	.5777	.6464	$\bar{f}$
12.0	215.3	193.5	188.3	181.3	173.8	190.4
10.0	214.0	198.6	188.1	179.4	176.6	191.3
8.0	217.2	204.3	193.7	184.4	174.6	194.8
6.0	231.3	212.7	202.5	194.9	187.2	205.6
4.0	247.9	227.3	219.2	199.2	198.4	218.3
2.0	266.1	247.8	242.7	234.6	222.2	242.6
		C(M,f) = R/Mf, in count/sec-Kg[a]				$C(M,\bar{f})$ C/Sec-Kg[b]
$\bar{M}$	232.0	214.0	205.8	195.7	188.8	
		$\overrightarrow{C(M,f)}$, in C/sec-Kg[c]				

a) Calculated from results in Table I

b) Plotted vs M in Figure 8

c) Plotted vs f in Figure 9

TABLE III. C_o FOR U_3O_8 MEASUREMENTS[a]

M=mass U_3O_8 (Kg)	f = weight fraction of ^{235}U				
	.3285	.4106	.4940	.5777	.6464
12.0	154.8	149.5	154.1	155.3	153.3
10.0	152.1	151.6	152.2	151.9	153.9
8.0	151.2	152.8	153.5	152.9	149.1
6.0	155.2	153.4	154.7	155.8	154.1
4.0	156.0	153.7	157.1	149.3	153.1
2.0	150.2	150.3	156.0	157.8	153.9

C_o, in C/sec-Kg $\qquad$ $\bar{C}_o = 153.3 \pm 0.4$

a) C_o calculated with equation (5b), using C(M,f) from Table II.

TABLE IV. $(C_o-\bar{C}_o)$ FOR U_3O_8 MEASUREMENTS[a]

M=mass U_3O_8 (Kg)	f=weight fraction of ^{235}U .3285	.4106	.4940	.5777	.6464	$\bar{f}$
12.0	1.0	-2.5	0.5	1.3	-0.0	-0.1 ±1.4
10.0	-0.8	-1.1	-0.7	-0.9	0.4	-0.6 ±0.5
8.0	-1.4	-0.3	0.2	-0.2	-2.7	-0.9 ±1.1
6.0	1.2	0.0	0.9	1.6	0.5	0.8 ±0.6
4.0	1.8	0.3	2.5	-2.6	-0.1	0.4 ±1.8
2.0	-2.0	-1.9	1.8	2.9	0.4	0.2 ±2.0
	$C_o - \bar{C}_o$, in %					DC_o $\pm\sigma(DC_o)$
$\bar{M}$	0.0 ±1.4	-0.9±0.9	0.9±0.9	0.4 ±1.8	-0.3±1.1	

a) $C_o-\bar{C}_o$ in % of $\bar{C}_o$, using data of Table III. Note: these deviations are the same as R-R(fit), where R(fit) is given by equation (5).

TABLE V. STATISTICAL ANALYSIS FOR 6 Kgm U_3O_8 MEASUREMENTS[a]

f	Series	$\bar{R}$(Sec^{-1})	n[b]	σ_T(1%)	ρ(<1%)[c]	ρ(<2%)	ρ(<3%)
0.3285	E	454.95	8	0.64	0.88	1.00	1.00
	F	456.63	7	0.78	0.80	0.99	1.00
	E&F	455.7	15	0.71	0.84	1.00	1.00
0.4106	E	524.09	8	0.79	0.79	0.99	1.00
	F	523.98	7	0.60	0.90	1.00	1.00
	E&F	524.0	15	0.69	0.85	1.00	1.00
0.4940	E	600.19	7	0.43	0.98	1.00	1.00
	F	600.35	7	0.64	0.88	1.00	1.00
	E&F	600.3	14	0.52	0.94	1.00	1.00
0.5777	E	676.42	7	0.95	0.71	0.96	1.00
	F	674.61	7	0.83	0.77	0.98	1.00
	E&F	675.5	14	0.87	0.75	0.97	1.00
0.5777[d]	E	677.01	5	0.50	0.95	1.00	1.00
	F	676.36	5	0.61	0.90	1.00	1.00
	E&F	676.7	10	0.53	0.93	1.00	1.00
0.6464	E	728.07	7	0.36	0.99	1.00	1.00
	F	723.91	9	0.62	0.89	1.00	1.00
	E&F	726.0	16	0.58	0.92	1.00	1.00
0.6464[d]	E	728.07	7	0.36	0.99	1.00	1.00
	F	725.24	7	0.30	1.00	1.00	1.00
	E&F	726.7	14	0.37	0.99	1.00	1.00

a) Refer to Appendix Table A.4 for detailed data.
b) n=number of measurements used to calculate $\bar{R}$ and σ_T. (See equation (5).)
c) $\rho(\varepsilon)$ is probability that a single measurement will be within $\pm\ \varepsilon$ of true value, where

$$\rho(\varepsilon) = \frac{1}{\sqrt{2\pi}} \int_{-\varepsilon}^{\varepsilon} e^{-x^2/2\sigma_T} dx$$

d) Suspicious measurements deleted.

Figure 1. Active Well Coincidence Counter.

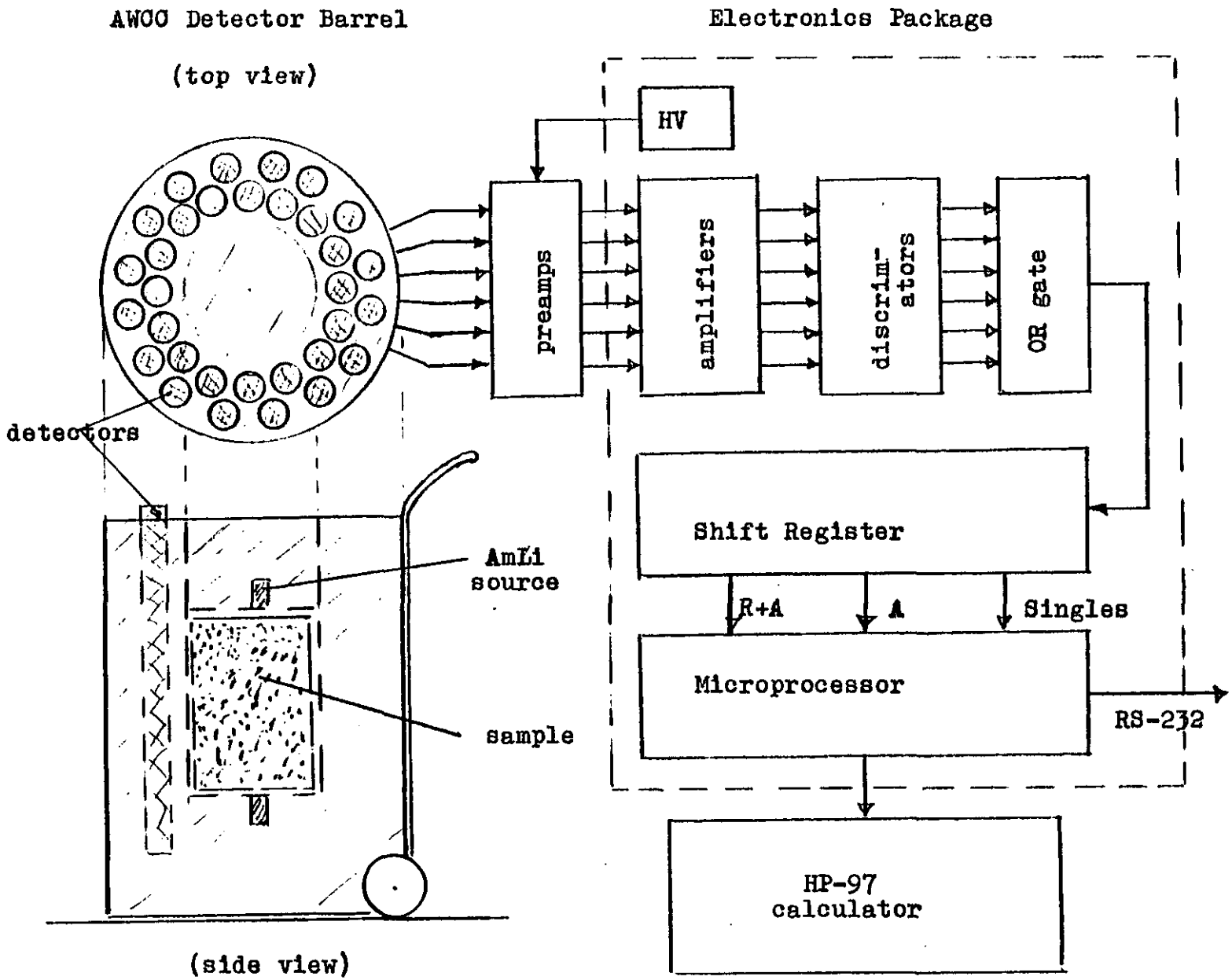

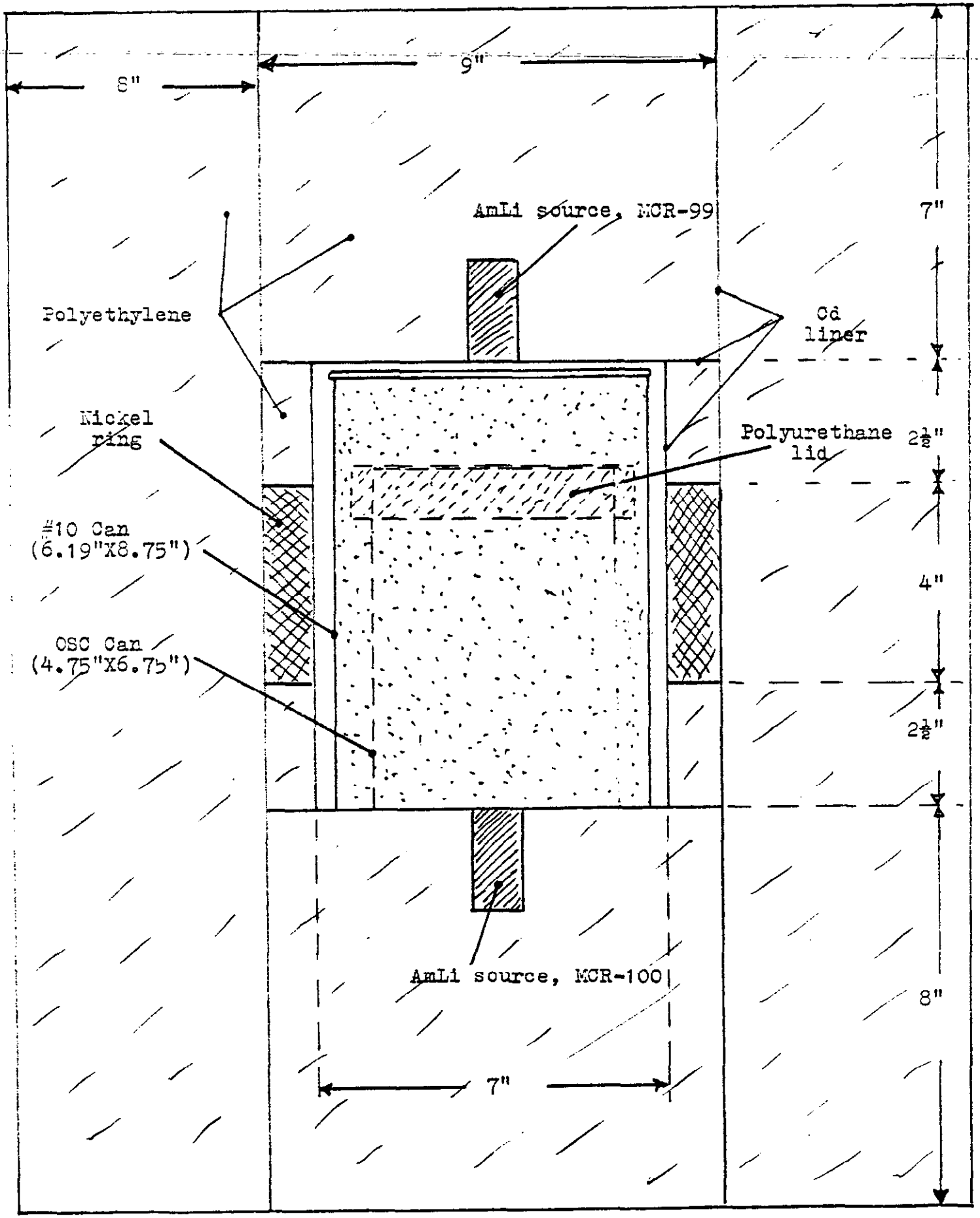

Figure 2. AWCC geometry for scoping studies on U_3O_8.

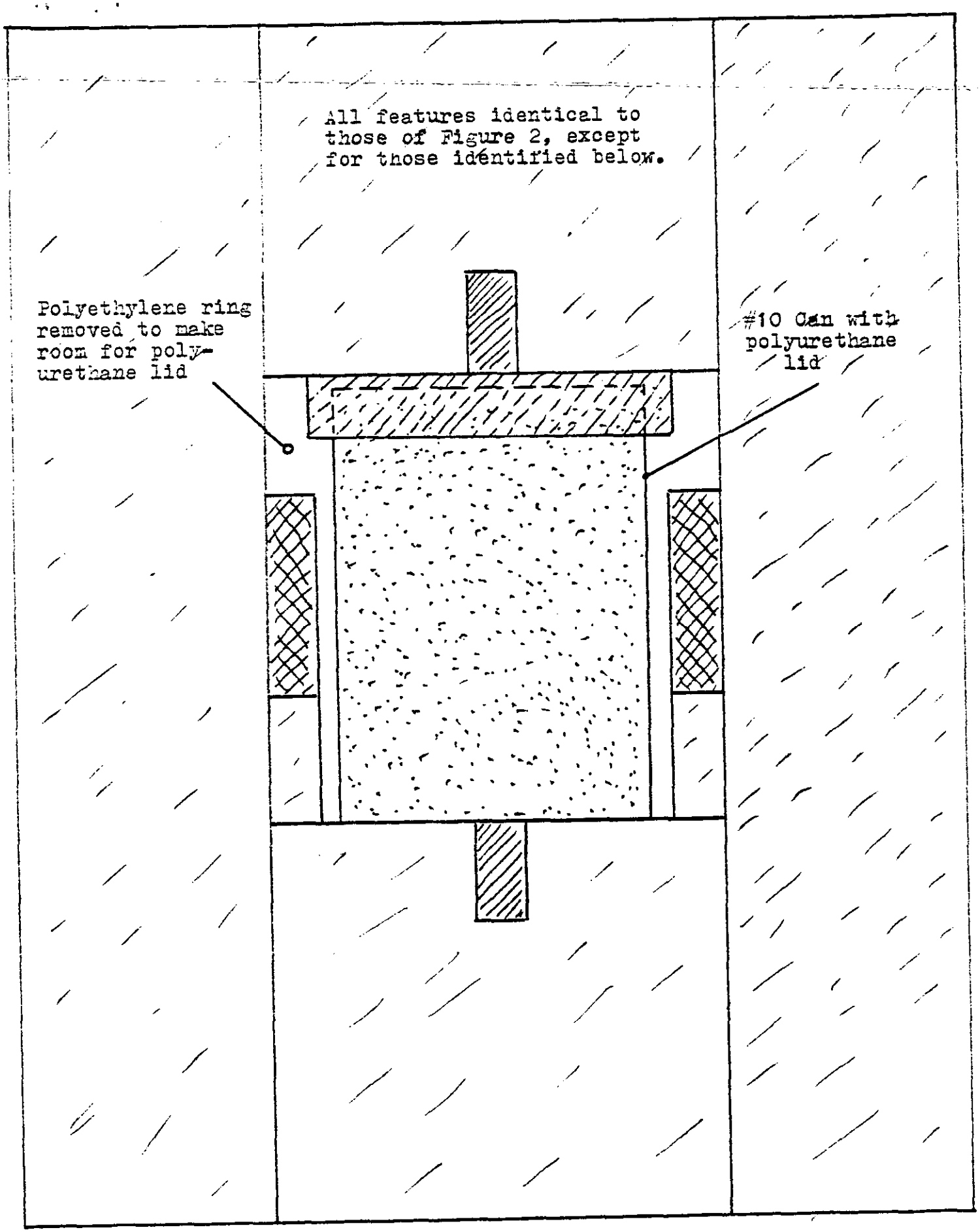

Figure 3. AWCC counting geometry for detailed studies on U308.

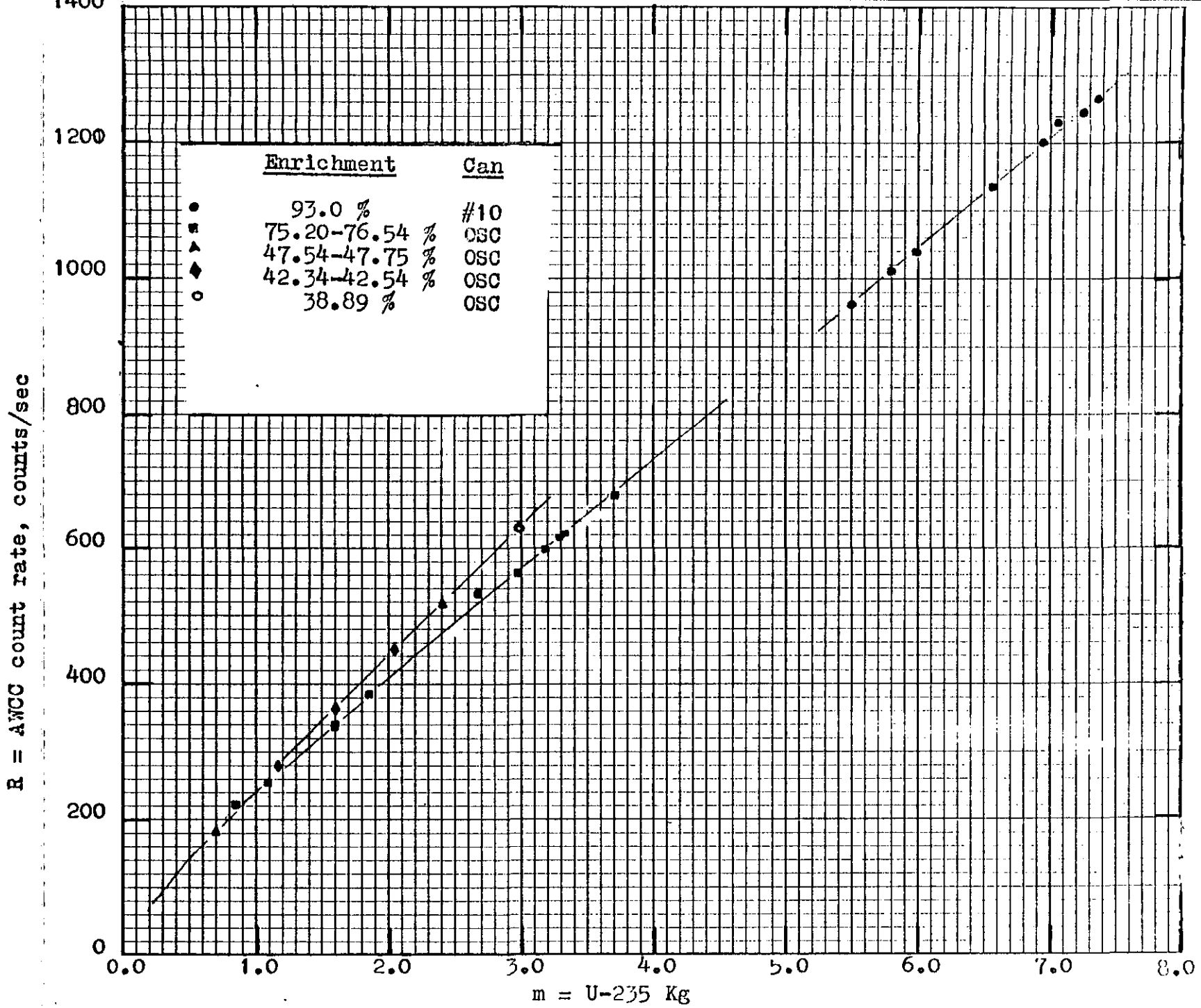

Figure 4. R vs m for U_3O_8 scoping studies.

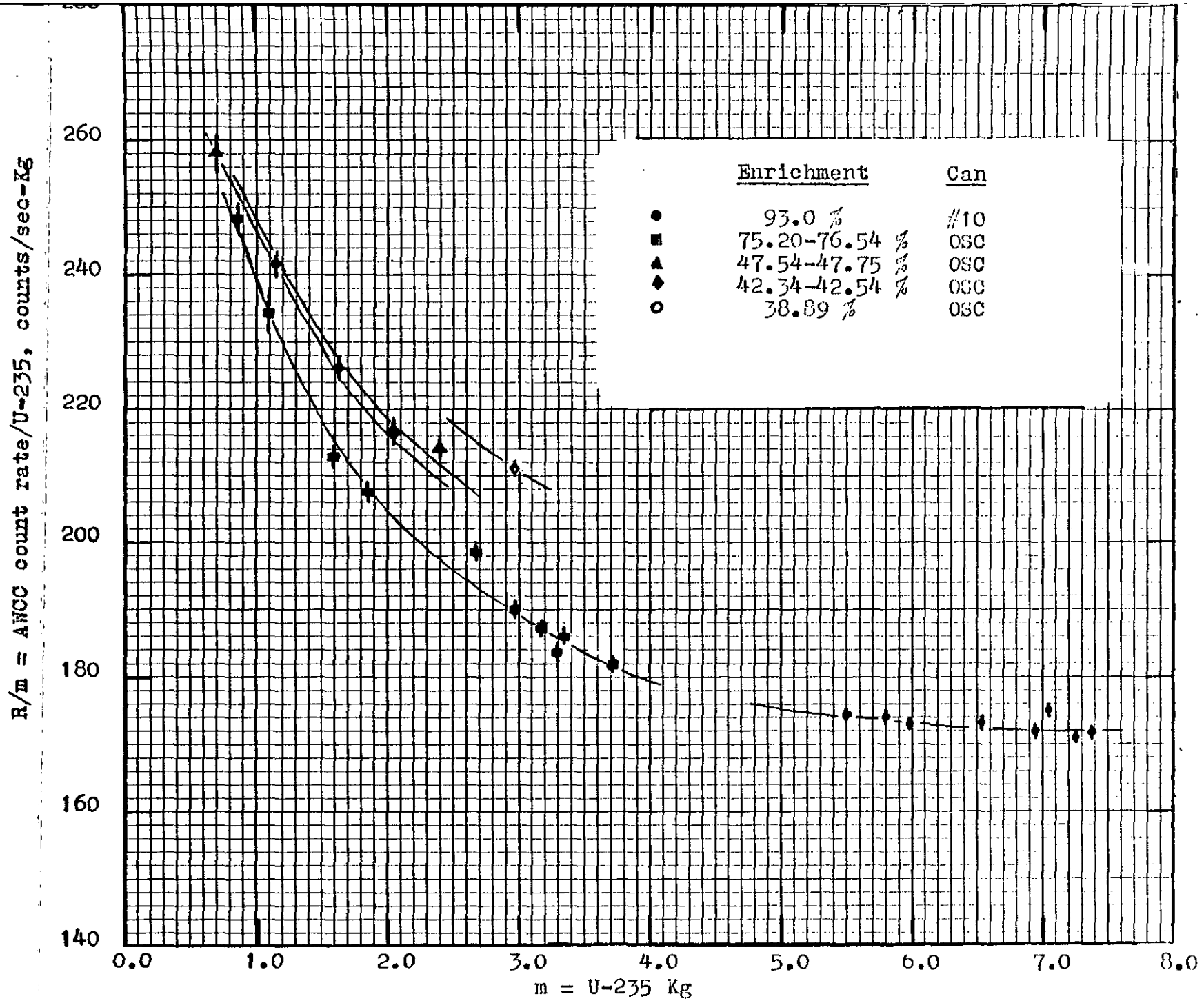

Figure 5. R/m vs m for U308 scoping studies.

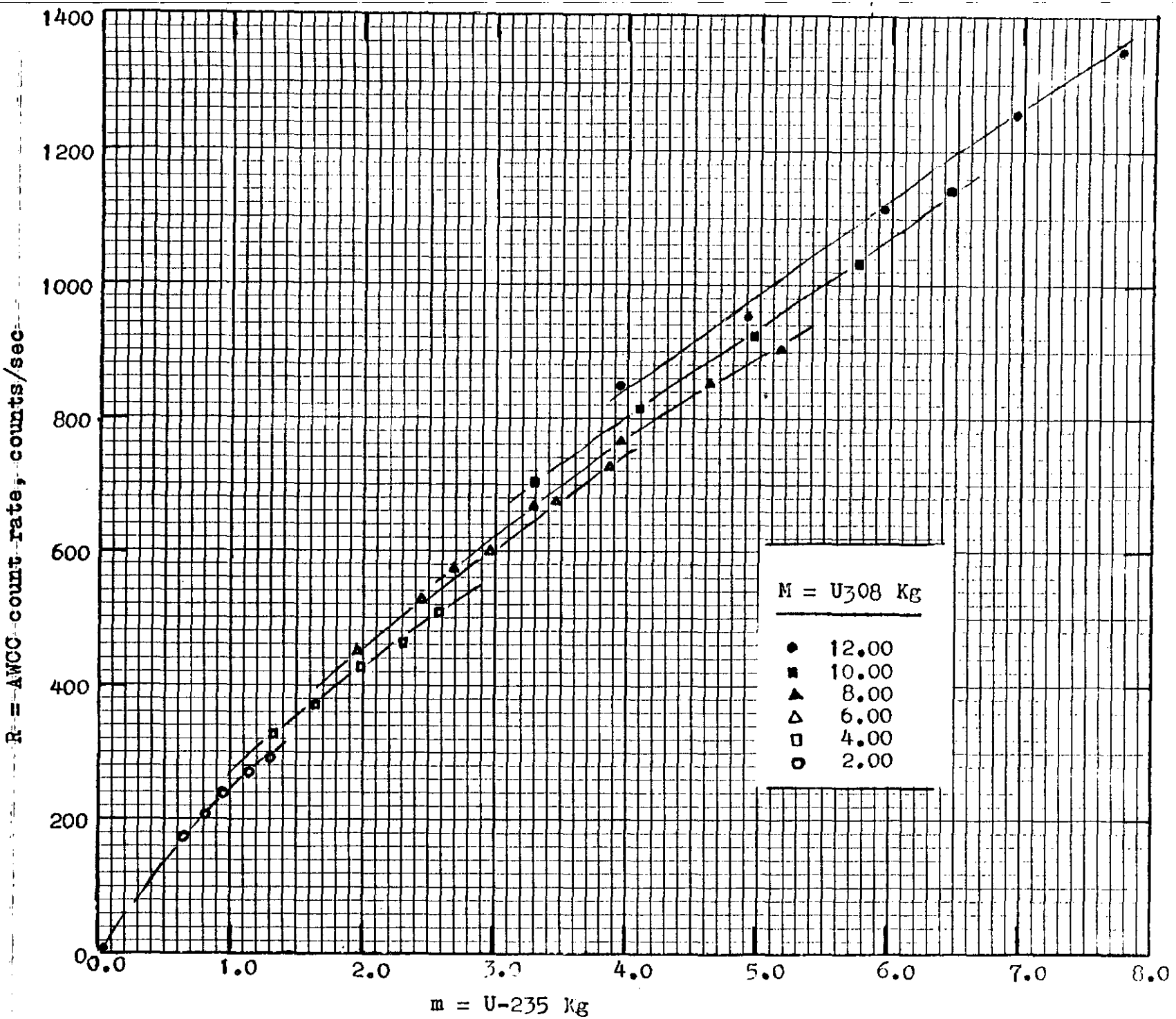

Figure 6. R vs m for detailed studies with #10 Cans.

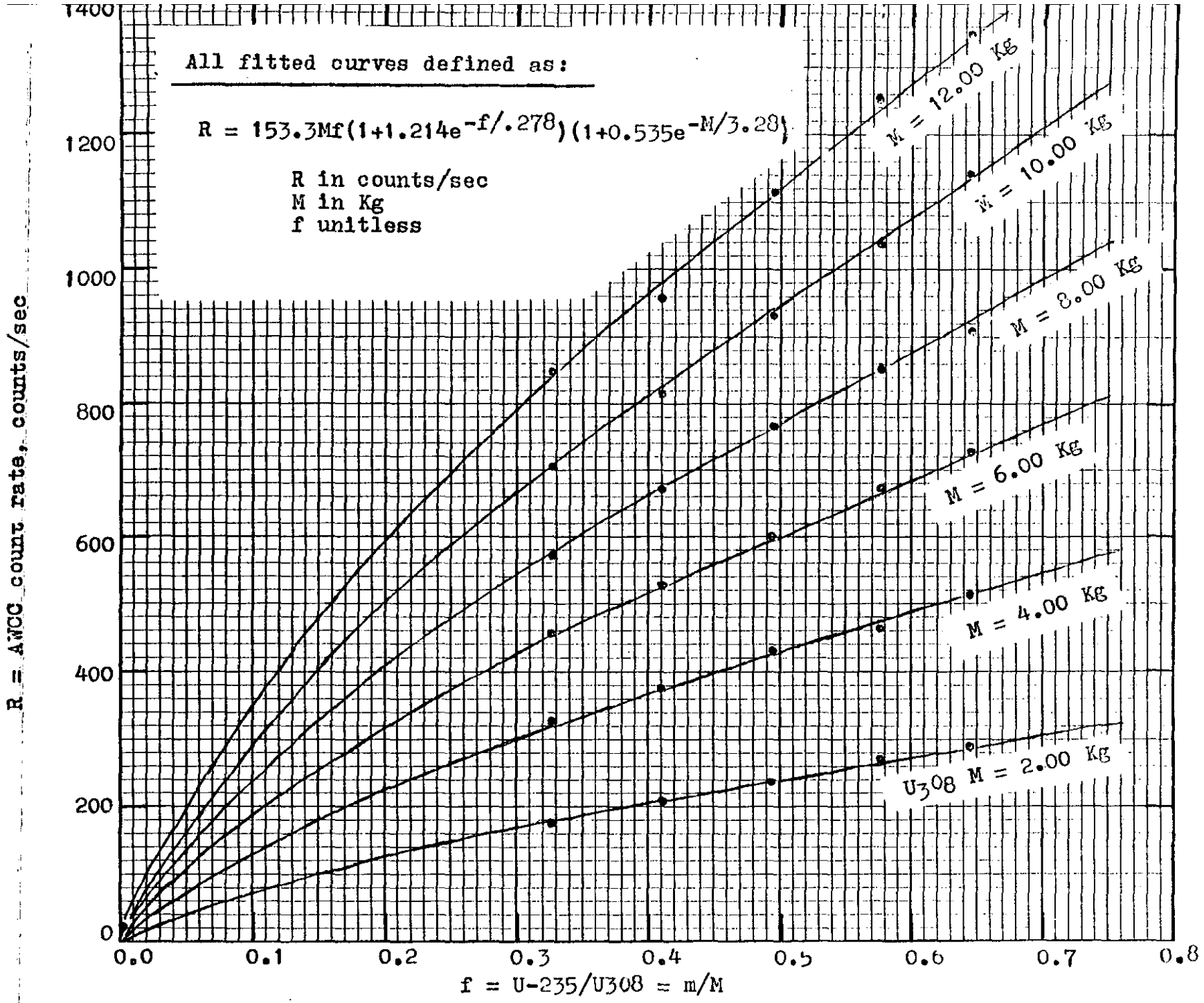

Figure 7. R vs f for detailed studies with #10 Cans.

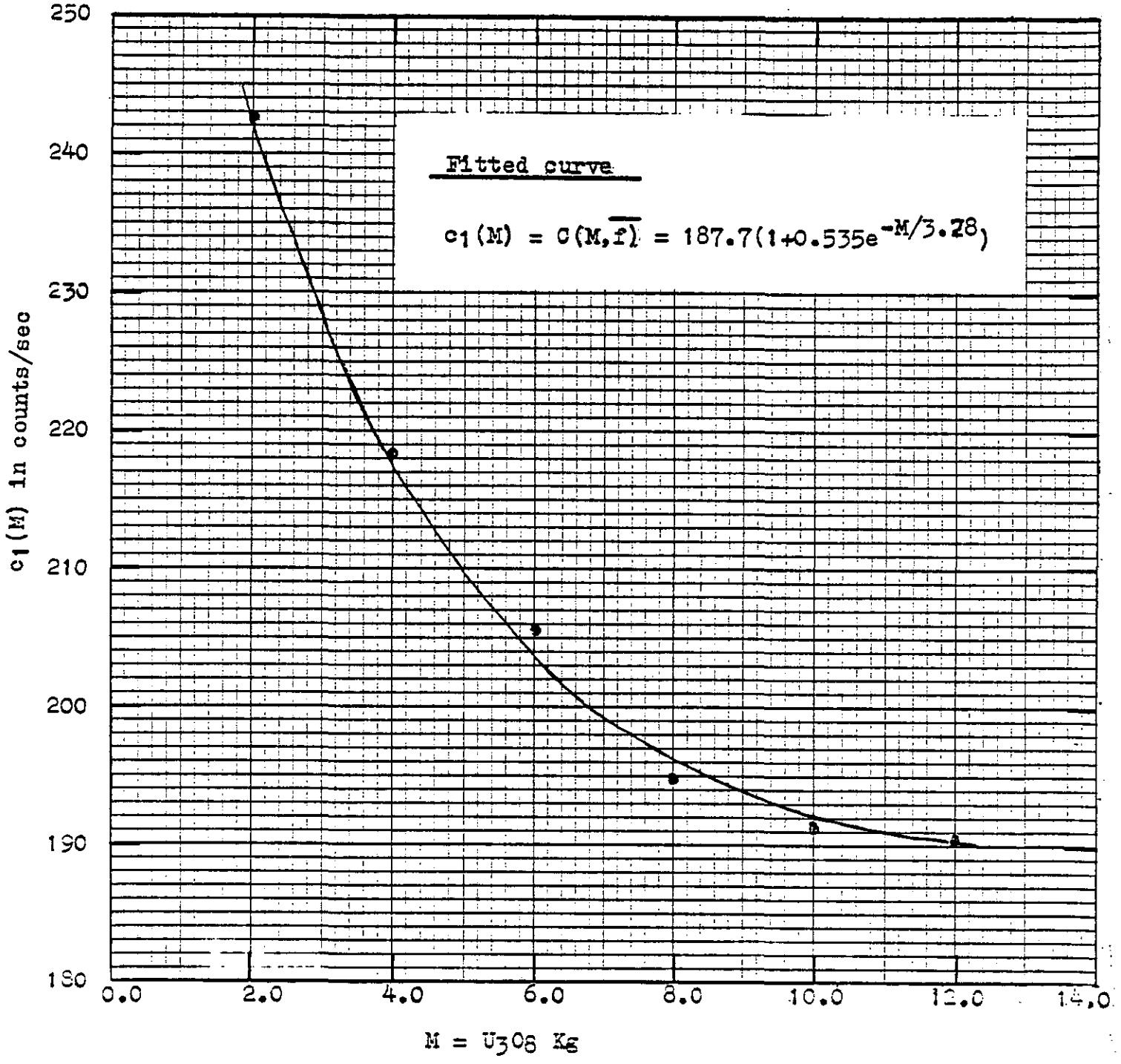

Figure 8. $c_1(M)$ vs M from detailed U_3O_8 studies.

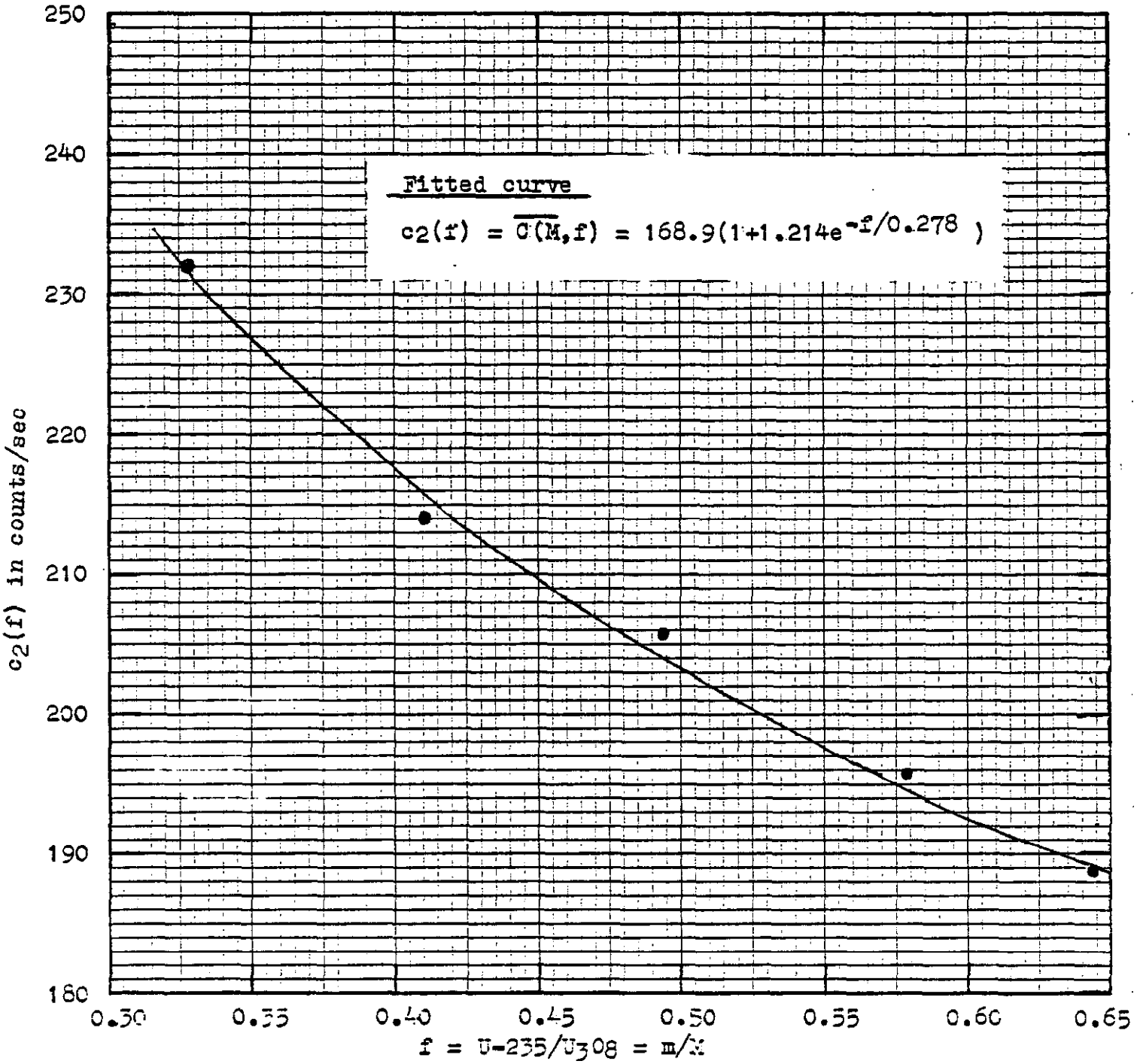

Figure 9. $c_2(f)$ vs f for detailed U_3O_8 studies.

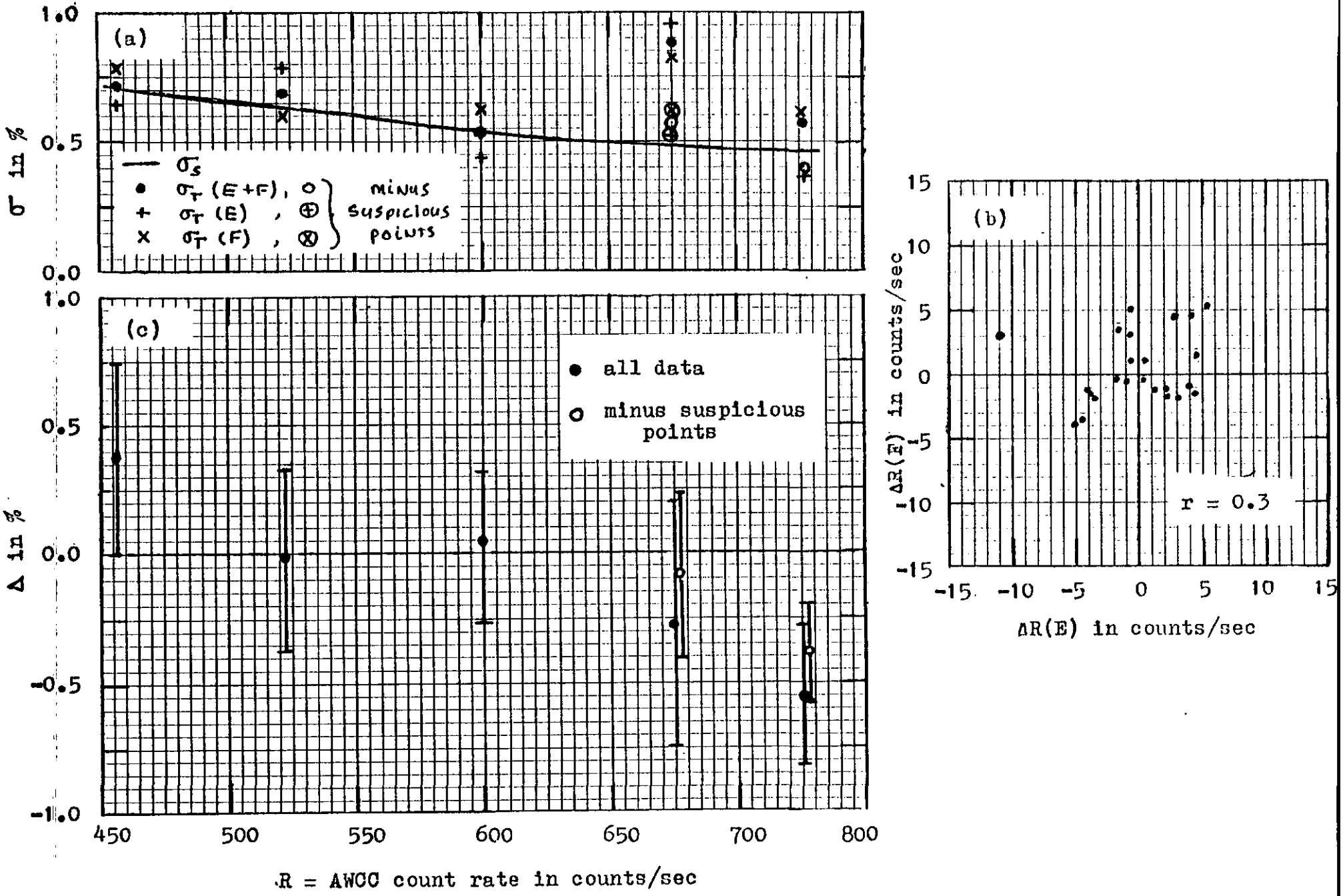

Figure 10. Errors in R for detailed U_3O_8 measurements with M = 6.00 Kg: (a) σ_T vs σ_S comparisons, (b) correlation coefficient analysis, (c) comparison of "identical" samples.

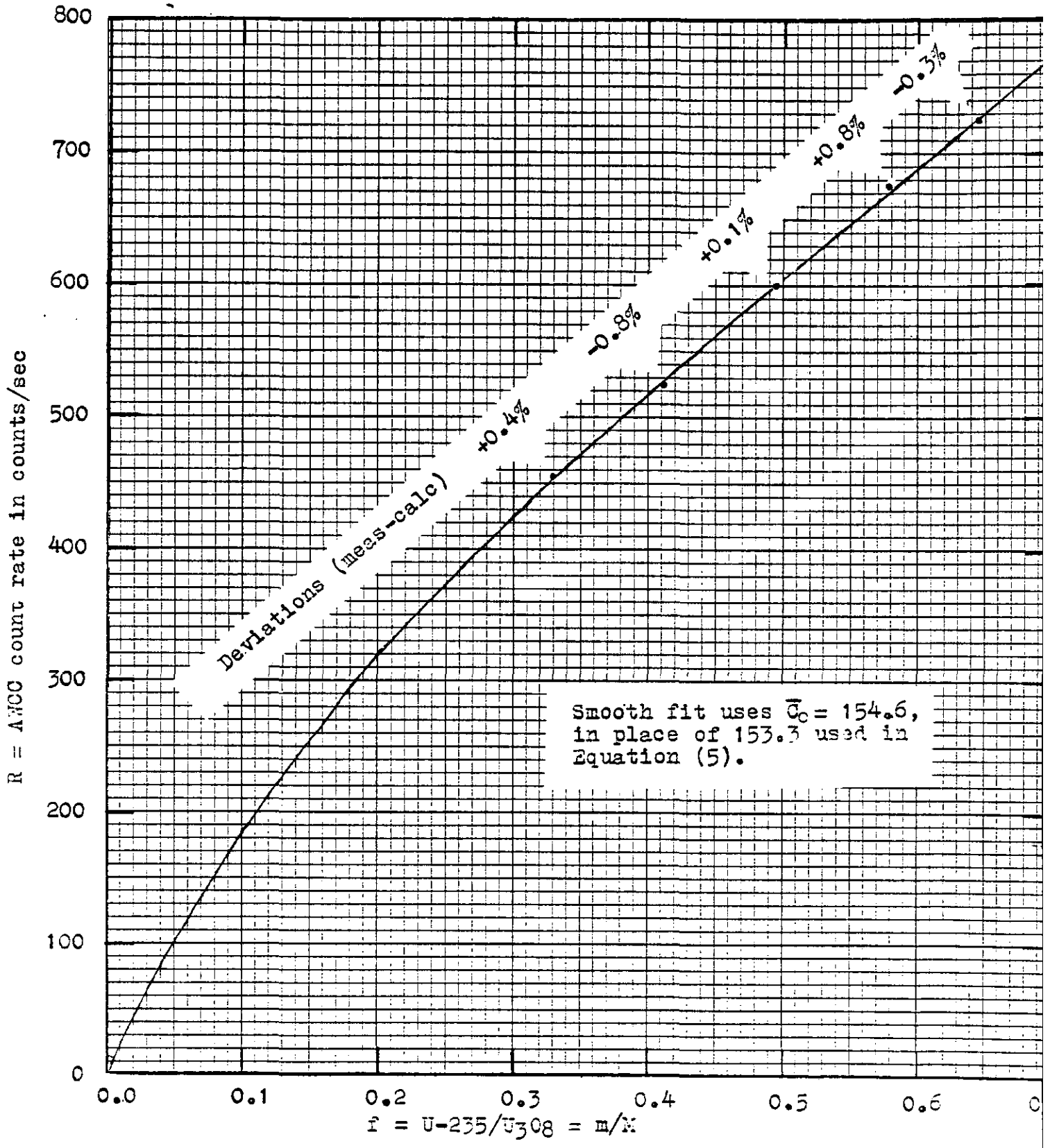

Figure 11. R vs f for #10 Cans with M = 6.00 Kg.

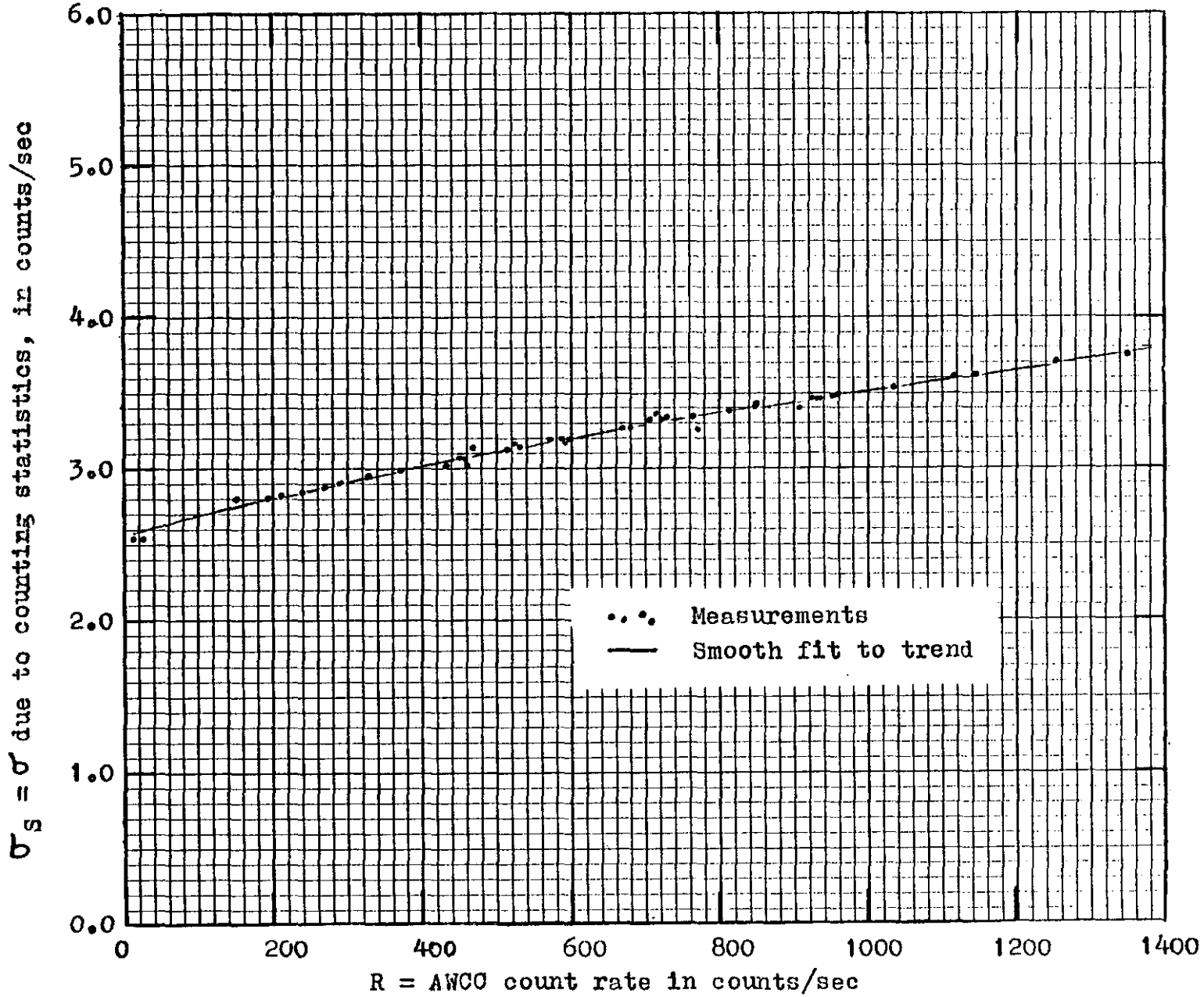

Figure 12. σ_S vs R for AWCO measurements, with 2000 sec count times.

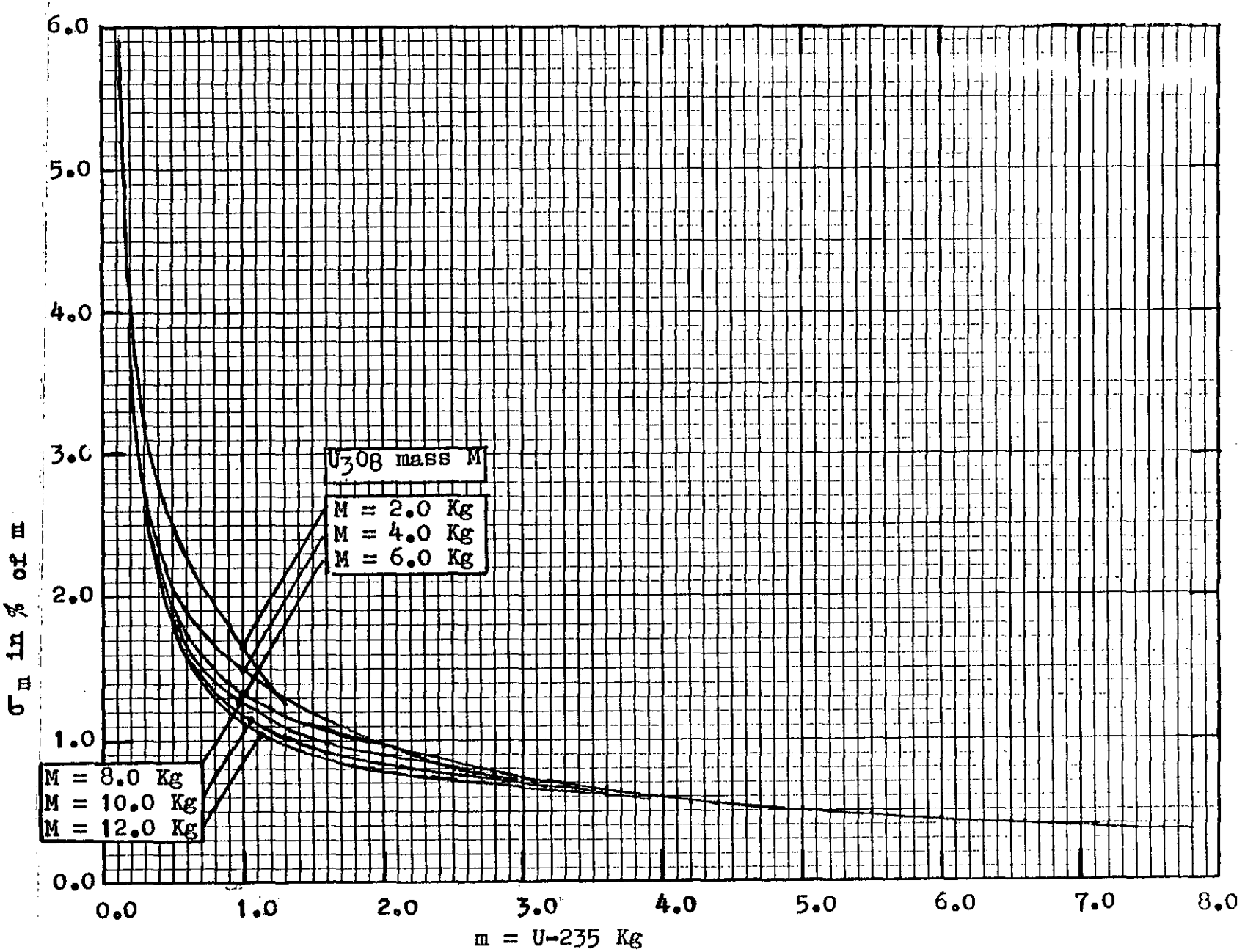

Figure 13. σ_m vs m, assuming 2000 sec count time and $\sigma_R = \sigma_S$.

APPENDIX. AWCC DATA

Data taken in these studies are presented for the convenience of other AWCC researchers. A guide for using these tables is presented below:

All Data Tables

- R is given in counts per sec statistical counting error σ_S.
- Count times for R measurements are given as n x ti, where n individual count intervals of duration ti are summed for the total count time.

Tables A.1 and A.2

- Data from Scoping Studies

Table A.3

- Data from Detailed Studies
- f = wt ^{235}U/wt U_3O_8

Table A.4

- Data for extensive 6.0 Kg sample tests
- f = wt ^{235}U/wt U_3O_8
- Series refer to one of two "identical" 6.0 Kg samples

  E, F } denotes two different samples

  E+F $\bar{R}$, etc. based on both E and F

  E,F $\bar{R}$ estimated as $[\bar{R}(E) + \bar{R}(F)]/2$

- Date refers to time of measurement

- Analysis insert boxes

  $\bar{R}$ average R

  σ_S counting error of R

  $\bar{\sigma}_S$ counting error of $\bar{R}$

  σ_T measured standard deviation for R

  $\bar{\sigma}_T$ measured standard deviation for $\bar{R}$

  $\Delta = (\bar{R} \pm \bar{\sigma}_T)_F - (\bar{R} \pm \bar{\sigma}_T)_E$

Tables A.5 and A.6

- Data for New Brunswick Samples/Scrap Samples-300 Area
- Sample mass is used as M in analyses

TABLE A.1 SCOPING STUDIES-#10 CANS (SEALED-NO POLYURETHANE LID)

^{235}U Enrichment %	U_3O_8 Kg	^{235}U Kg	R c/s	Count Time nxti, sec
93	6.995	5.493	959.0±2.7	6x500
93	7.370	5.807	1010.9±4.6	2x500
93	7.608	5.982	1038.9±6.6	2x500
93	8.347	6.570	1134.7±4.8	2x500
93	8.834	6.741	1195.5±4.8	2x500
93	8.954	7.040	1230.4±4.8	2x500
93	9.210	7.268	1242.9±4.9	2x500
93	9.368	7.372	1265.4±4.9	2x500

TABLE A.2 SCOPING STUDIES - OSC CANS

^{235}U Enrichment	U_3O_8	^{235}U	R	Count Time
%	Kg	Kg	c/s	nxti, sec
38.87	9.085	2.982	629.3±3.3	3x500
42.34	3.265	1.167	281.8±2.4	4x500
42.36	5.772	2.065	448.1±2.8	4x500
42.54	4.498	1.619	366.7±1.9	8x500
47.45	1.744	0.699	180.6±2.3	4x500
47.45	5.980	2.414	517.4±3.1	3x500
75.20	2.970	1.855	385.1±2.6	4x500
75.47	1.359	0.851	211.4±1.7	8x500
75.50	4.753	2.976	565.4±3.2	3x500
75.51	4.285	2.684	532.4±3.1	3x500
75.94	2.503	1.596	339.9±2.5	4x500
75.94	4.995	3.185	597.4±3.3	3x500
75.94	5.219	3.328	620.1±3.3	3x500
76.54	1.690	1.092	256.2±3.4	2x500
76.54	5.104	3.298	613.1±4.1	2x500
76.54	5.766	3.726	678.5±3.0	4x500

TABLE A.3 DETAILED STUDIES-#10 CANS (WITH POLYURETHANE LID)

U_3O_8	^{235}U	f	^{235}U Enrichment	R	Count Time
Kg	Kg	#	%	c/s	nxti,sec
2.000	0.657	0.3285	38.89	174.8±2.8	4x500
2.000	0.821	0.4106	48.61	203.5±2.0	8x500
2.000	0.988	0.4940	58.65	239.8±2.8	4x500
2.000	1.155	0.5777	68.71	271.1±2.9	4x500
2.000	1.292	0.6464	76.54	287.2±2.9	4x500
3.999	1.314	0.3285	38.89	325.8±2.4	8x500
4.000	1.642	0.4106	48.61	373.3±2.5	4x500
4.003	1.976	0.4940	58.65	433.2±3.0	4x500
4.000	2.311	0.5777	68.71	460.3±3.0	4x500
4.000	2.585	0.6464	76.54	512.9±3.1	4x500
5.998	1.971	0.3285	38.89	455.8±0.8	many[a]
5.999	2.463	0.4106	48.61	524.0±0.8	many[a]
6.000	2.964	0.4940	58.65	600.3±0.9	many[a]
6.000	3.464	0.5777	68.71	675.5±0.9	many[a]
6.000	3.877	0.6464	76.54	726.0±0.8	many[a]

a) See Table A.4 for details

TABLE A.3 (CONT'D)

U_3O_8	^{235}U	f	^{235}U Enrichment	R	Count Time
Kg	Kg	#	%	c/s	nxti,sec
7.998	2.628	0.3285	38.89	570.8±2.0	11x500
7.998	3.284	0.4106	48.61	671.1±3.3	4x500
8.003	3.940	0.4940	58.65	765.5±3.3	4x500
7.999	4.621	0.5777	68.71	852.1±3.4	4x500
8.000	5.170	0.6464	76.54	903.1±3.4	4x500
10.000	3.285	0.3285	38.89	703.0±3.3	4x500
10.000	4.106	0.4106	48.61	815.3±3.4	4x500
10.003	4.942	0.4940	58.65	929.2±2.4	8x500
10.000	5.777	0.5777	68.71	1036.5±3.5	4x500
10.000	6.462	0.6464	76.54	1141.3±3.6	4x500
12.000	3.942	0.3285	38.89	848.9±3.4	4x500
12.000	4.927	0.4106	48.61	953.6±2.5	8x500
12.003	5.929	0.4940	58.65	1116.3±3.6	4x500
12.000	6.933	0.5777	68.71	1257.1±3.7	4x500
12.000	7.754	0.3285	76.54	1348.2±3.7	4x500
12.000	0.0173	0.0014	0.17	20.4±1.8	8x500

TABLE A.4 EXTENSIVE TESTS WITH 6 Kg SAMPLES

^{235}U Enrich. %	f #	^{235}U Kg	Series	R c/s	Count Time nxti,sec	Date m/d/81
38.89	0.3285	1.971	E	454.5±3.1	4x500	5/8
			E	455.6±3.1	4x500	5/13
			E	453.7±3.1	4x500	5/19
			E	458.1±3.1	4x500	5/20
			E	450.0±3.1	1x2000	6/4
			E	452.4±3.1	1x2000	6/4
			E	456.7±3.2	1x2000	6/10
			E	458.6±3.2	1x2000	6/10
			F	461.5±3.1	4x500	5/8
			F	457.6±3.1	4x500	5/13
			F	460.2±3.1	4x500	5/19
			F	453.2±3.1	1x2000	6/4
			F	455.6±3.1	1x2000	6/4
			F	457.0±3.2	1x2000	6/10
			F	451.4±3.2	1x2000	6/10

ANALYSIS

Series	$\bar{R}$	σ_S	$\bar{\sigma}_S$	σ_T	$\bar{\sigma}_T$
E	454.95	3.13	1.11	2.92	1.03
F	456.63	3.13	1.19	3.58	1.35
E&F	455.7	3.13	0.81	3.25	0.84
$\overline{E,F}$	455.8				

$\Delta = (\bar{R} \pm \bar{\sigma}_T)_F - (\bar{R} \pm \bar{\sigma}_T)_E$

$= 1.68 \pm 1.69$

^{235}U Enrich. %	f #	^{235}U Kg	Series	R c/s	Count Time nxti,sec	Date m/d/81
48.61	0.4106	2.463	E	530.2±3.1	4x500	5/7
			E	529.5±3.1	4x500	5/8
			E	521.8±3.2	4x500	5/13
			E	525.0±3.2	4x500	5/19
			E	518.0±3.2	1x2000	5/28
			E	523.2±3.2	1x2000	5/28
			E	524.2±3.2	1x2000	6/10
			E	520.9±3.2	1x2000	6/10
			F	529.3±3.1	4x500	5/8
			F	519.3±3.1	4x500	5/13
			F	523.9±3.2	4x500	5/19
			F	523.6±3.2	1x2000	6/2
			F	525.0±3.2	1x2000	6/2
			F	525.3±3.2	1x2000	6/10
			F	521.5±3.2	1x2000	6/10

ANALYSIS

Series	$\bar{R}$	σ_S	$\bar{\sigma}_S$	σ_T	$\bar{\sigma}_T$
E	524.09	3.18	1.12	4.15	1.46
F	523.98	3.18	1.20	3.17	1.20
E&F	524.0	3.18	0.82	3.59	0.93
$\overline{E,F}$	524.0				

$\Delta = (\bar{R} \pm \bar{\sigma}_T)_F - (\bar{R} \pm \bar{\sigma}_T)_E$

$= 0.11 \pm 1.89$

TABLE A.4 (CONT'D)

^{235}U Enrich.	f	^{235}U
%	#	Kg
58.65	0.4940	2.964

ANALYSIS

Series	$\bar{R}$	σ_S	$\bar{\sigma}_S$	σ_T	$\bar{\sigma}_T$
E	600.19	3.22	1.22	2.61	0.99
F	600.35	3.22	1.22	3.88	1.47
E&F	600.3	3.22	0.86	3.17	0.84
$\overline{E,F}$	600.3				

$\Delta = (\bar{R} \pm \bar{\sigma}_T)_F - (\bar{R} \pm \bar{\sigma}_T)_E$

$= 0.16 \pm 1.77$

^{235}U Enrich.	f	^{235}U
%	#	Kg
68.71	0.5777	3.464

ANALYSIS

Series	$\bar{R}$	σ_S	$\bar{\sigma}_S$	σ_T	$\bar{\sigma}_T$
E	676.42	3.34	1.26	6.45	2.44
F	674.61	3.34	1.26	5.62	2.12
E&F	675.5	3.34	0.89	5.89	1.57
$\overline{E,F}$	675.5				

$\Delta = (\bar{R} \pm \bar{\sigma}_T)_F - (\bar{R} \pm \bar{\sigma}_T)_E$

$= -1.81 \pm 3.23$

Minus 6/9 Measurements

E	677.01	3.34	1.36	3.37	1.38
F	676.36	3.34	1.36	4.14	1.69
E&F	676.7	3.34	0.96	3.58	1.13
$\overline{E,F}$	676.7				

$\Delta = 0.65 \pm 2.18$

Series	R	Count Time	Date
	c/s	nxti,sec	m/d/81
E	598.1±3.2	4x500	5/7
E	600.0±3.2	4x500	5/14
E	604.9±3.2	4x500	5/18
E	602.2±3.2	1x2000	6/2
E	597.6±3.2	1x2000	6/2
E	598.4±3.3	1x2000	6/8
E	600.2±3.3	1x2000	6/8
F	596.9±3.2	4x500	5/7
F	600.8±3.2	4x500	5/14
F	603.1±3.2	4x500	5/18
F	593.7±3.2	1x2000	6/3
F	605.3±3.2	1x2000	6/3
F	601.6±3.3	1x2000	6/10
F	601.0±3.3	1x2000	6/10
E	672.5±3.3	4x500	5/7
E	680.9±3.3	4x500	5/14
E	674.7±3.3	4x500	5/18
E	677.8±3.3	1x2000	6/3
E	679.1±3.4	1x2000	6/3
E	684.9±3.4	1x2000	6/9
E	665.0±3.4	1x2000	6/9
F	669.1±3.3	4x500	5/7
F	678.1±3.3	4x500	5/14
F	678.0±3.3	4x500	5/18
F	679.4±3.3	1x2000	6/4
F	677.3±3.4	1x2000	6/4
F	664.4±3.4	1x2000	6/9
F	676.0±3.4	1x2000	6/9

TABLE A.4 (CONT'D)

^{235}U Enrich.	f	^{235}U
%	#	Kg
75.54	0.6464	3.877

Series	R	Count Time	Date
	c/s	nxti,sec	m/d/81
E	731.0±3.3	4x500	5/7
E	731.1±3.3	4x500	5/13
E	727.4±3.3	4x500	5/19
E	724.6±3.4	1x2000	6/3
E	729.6±3.4	1x2000	6/3
E	725.2±3.4	1x2000	6/10
E	727.6±3.4	1x2000	6/10
F	713.3±3.3	4x500	5/7
F	723.5±3.4	4x500	5/13
F	723.7±3.3	4x500	5/14
F	727.2±3.3	4x500	5/18
F	722.4±3.3	4x500	5/19
F	727.6±3.4	1x2000	6/3
F	726.7±3.4	1x2000	6/3
F	723.5±3.4	1x2000	6/9
F	727.4±3.4	1x2000	6/9

ANALYSIS

Series	$\bar{R}$	σ_S	$\bar{\sigma}_S$	σ_T	$\bar{\sigma}_T$
E	728.07	3.36	1.27	2.61	0.99
F	723.91	3.36	1.12	4.47	1.49
E&F	725.7	3.36	0.84	4.23	1.06
$\overline{E,F}$	726.0				

$\Delta = -4.16 \pm 1.79$

MINUS 6/9 F MEASUREMENT

E	728.07	3.36	1.27	2.61	0.99
F	725.24	3.36	1.18	2.14	0.75
E&F	726.6	3.36	0.87	2.72	0.70
$\overline{E,F}$	726.7				

$\Delta = -2.83 \pm 1.3$

TABLE A.5 NEW BRUNSWICK SAMPLES

Sample Mass	Count Rate, R [a]	Count Time	^{235}U		
			Calc	Known	Calc-Known
Kg	c/s	nxti,sec	Kg	Kg	%
0.950	-4.4±3.2 [b]	1x2000	-0.009±0.007	0.0	
	3.2±3.2	1x2000	0.007±0.007		
	-9.8±3.2 [b]	1x2000	-0.021±0.007		
	-3.7±1.9 [b]	3x2000	-0.008±0.004		
	±6.5		±0.014		
0.950	45.4±3.3	1x2000	0.119±0.011	0.12535	-5.1±8.7
	56.5±3.2	1x2000	0.158±0.012	"	26.0±9.6
	53.0±3.2	1x2000	0.145±0.011	"	15.7±8.7
	51.6±2.0	3x2000	0.140±0.007	"	11.6±5.6
	±5.7		±0.020		±15.9

a) First error is σ_S. If a second error exists, it is σ_T.

b) Negative count rate due to fluctuation about zero in (seals + randoms) - (randoms) calculation.

TABLE A.6 SCRAP SAMPLES FROM 300-AREA

Sample Mass(Net)	Count Rate,R [a]	Count Time	^{235}U		
			Calc	Known	Calc-Known
Kg	c/s	nxti,sec	Kg	Kg	%
5.998	529.1±2.8 ±2.3	5x500	2.502±0.016 ±0.013	2.463	1.6±0.7 ±0.5
2.542	136.1±1.7 ±5.2	4x2000	0.429±0.006 ±0.022	0.42196	1.7±1.4 ±5.1
2.284	120.2±1.7 ±0.7	4x2000	0.369±0.007 ±0.003	0.37542	-1.7±1.0 ±0.4
2.998	77.3±1.8 ±12.2	4x2000	0.214±0.006 ±0.039	0.34139	-37.4±1.8 ±11.4
3.246	59.8±1.7 ±18.2	4x2000	0.162±0.005 ±0.056	0.28417	-43.0±1.8 ±19.7
2.894	63.5±1.6 ±4.8	4x2000	0.171±0.005 ±0.014	0.21774	-21.5±2.3 ±6.4
1.358	38.9±1.6 ±12.9	4x2000	0.097±0.005 ±0.038	0.14233	-32.2±3.5 ±26.7
2.998	91.4±3.5[b]	1x2000	0.260±0.012	0.34139	-25.8±3.6
3.246	86.1±3.3[b]	1x2000	0.243±0.011	0.28417	-14.5±3.8
2.894	70.2±3.2[b]	1x2000	0.192±0.010	0.21774	-11.8±4.6
1.358	49.4±3.2[b]	1x2000	0.128±0.010	0.14233	-10.1±7.0

a) See footnote (a) in Table A.5

b) Most favorable measurements